Preparation of Acid Red73 adsorbed on chitosan-modified sepiolite with SiO_2 coating as a highly stable hybrid pigment

Xiayi (Eric) Hu[a,1,*], Xuechun Feng[a,1], Mingming Fei[a], Mi Tian[b], Rui Zhang[a], Yefeng Zhou[a,*], Yang Liu[c], Zhaogang Zeng[d]

[a] College of Chemical Engineering, Xiangtan University, Xiangtan 411105, P. R. China

[b] College of Engineering, Mathematics and Physical Sciences, University of Exeter, Exeter, EX44 PS, UK.

[c] Hunan BG Well-point Environmental Science & Technology Co., Ltd, Changsha 41000, P. R. China

[d] Xiangtan Sepiolite Technology Co., Ltd, Xiangtan 411100, P. R. China

*Corresponding Author: Xiayi (Eric) Hu E-mail address: xiayihu@xtu.edu.cn

*Corresponding Author**:** Yefeng Zhou E-mail address: zhouyf@xtu.edu.cn.

Tel & Fax: +86- 731-58298171

Abstract

The application of organic dyes in industry is severely limited due to its insolubility and instability. The adsorption of organic dyes by inorganic materials to form hybrid pigment is a valid method to improve its stability, thus widening its applications in industries. A simple method for preparing stable hybrid pigment by adsorpting Acid Red 73 (AR73) on the chitosan (CTS) modified sepiolite with a SiO_2 coating is explored in this work. Sepiolite modified by the CTS was used to immobilize AR73 (CTS-sep/AR73) uniformly to form a hybrid pigment. The effects of the dosage of CTS, the concentration of acetic acid (HAc) and the pH of AR73 solution for CTS-sep adsorption of AR73 were investigated. CTS-sep/AR73 was further coated with a layer of SiO_2 to form the CTS-sep/AR73@SiO_2 pigment, which enhanced the stabilities of the hybrid pigment. The CTS-sep/AR73@SiO_2 pigment shows excellent stability in strong acid, strong alkali and anhydrous ethanol environment, along with the improved thermal ageing, intensified UV resistance, and enhanced thermal stability (more than 220 ℃) which is higher than that of CTS-sep/AR73 hybrid pigment.

Keywords: sepiolite; chitosan; Acid Red 73; hybrid pigment; coating; stability

1. Introduction

Organic dyes have the advantages of a wide range of high color strength, excellent photosensitivity and colors compared with inorganic pigments [1, 2]. In addition, some of the organic dyes have been treated as a essectial material to manufacture textile, inks and electronic devices [1, 3]. However, the organic dyes still show the drawbacks in terms of the stability and undesirable solubility in different solvents [2]. Especially

under high temperature and ultraviolet conditions, the organic dyes show much lower stability than that of inorganic pigment [4]. The other important consideration for the organic dyes that cannot be neglected is the tendency to discolor in acidic or alkaline solutions [5]. Due to these drawbacks, organic dyes are rarely used in the field of coatings, which severely limited their application in industries as pigments. The aim of this work is to enhance the solubility and stability of the Acid Red73 dye and to explore the application of this organic dye as a pigment in industry.

The main way to enhance the insolubility and the stability of organic dyes in different solvents is to combine them with inorganic materials to form a hybrid pigment. There are three methods for preparing the hybrid pigments, inorganic core modification, adsorption of dyes onto inorganic materials and encapsulation of organic pigment with inorganic materials [6-8]. The most convenient method is to adsorb the dyes onto inorganic materials, such as SiO_2, TiO_2, sepiolite, and palygorskite [4, 6, 9-11]. Yang et al.[4] employed a coprecipitation method to prepare ZnAl layered double hydroxides and then to adsorb the Acid Blue 129 to prepare the hybrid pigment with the improved photostability. Zhang et al. [12] prepared the hybrid pigments which adsorb methylene blue on the natural palygorskite and the hybrid pigment had high stability. Wu et al. [11] prepared the inorganic/organic composite fluorescent pigment using the acid-activated-sepiolite, which has excellent stability. Furthermore, using inorganic materials to adsorb organic dyes to prepare hybrid pigments often rely on the inherent pore structure and the modified surface of inorganic materials [6]. Jesionowski et al. [13] prepared the highly stable hybrid pigment by adsorbing dye on aminosilane-treated silica surface.

As an low-cost and environmently friendly adsorbent, sepiolite has received widespread attention in recent years due to its unique structure, such as surface area, high porosity, abundant silanol, the uniform pore size and a negative charge on the surface [14]. Meanwhile, the sepiolite is also a natural clay mineral with low prices and abundant reserves [15]. The formation of hybrid pigments using sepiolite is one of the current development trend in the preparation of high stability hybrid pigments [11, 16, 17]. Chitosan (CTS) is a cellulose-like linear polycationic polysaccharide [18] which has a wide range of applications in different fields: biomedical purposes, cosmetics, photography, food and nutrition, etc. It contains the amine and hydroxyl functional side groups that allows CTS as a polyelectrolyte to compensate the negative charge of sepiolite [18-21]. The CTS modified sepiolite (CTS-sep) holds the characteristic framework of sepiolite but CTS enhances the capability of the material to adsorb species.

The C.I. Acid Red 73 (AR73), a kind of azo dye, is widely used in the industries of paper, timber, pharmaceutical, cement, textile and leather, etc. Figure 1 display the structural formulas of AR73. AR73 demonstrates a limited applications in acid and alkali situation when coated it as a pigment because of its poor thermal stability and low resilience in the harsh environment. In this work, AR73 molecules were adsorbed on CTS modified sepiolite to produce a CTS-sep organic-inorganic hybrid pigment. And then, a SiO_2 layer was introduced on the CTS-sep/AR73 hybrid pigment to further enhance its stability. In this work, we investigated the influences of CTS concentration, Acetic acid (HAc), pH on the stability of the AR73. In addition, we compared the

resistances and thermal stability between CTS-sep/AR73 and CTS-sep/AR73@SiO_2.

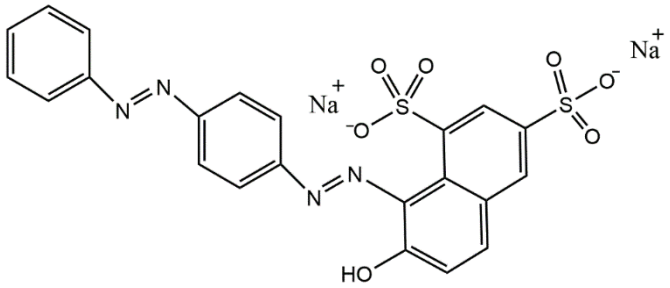

Figure 1. Molecular structure of AR73.

2. Materials and methods

2.1 Materials

The sepiolite was purchased from Hunan Xiangtan sepiolite technology Co.Ltd. AR73 ($C_{22}H_{14}N_4Na_2O_7S_2$) and TEOS (98%) were purchased from Macklin and Aladdin respectively. Acetic acid (HAc,99.5%), NaOH, HCl (37.5%), CTS (the degree of deacetylation is 80-95% and viscosity average are 50-800 mPa·s), anhydrous ethanol, Cetrimonium Bromide (CTAB), and ammonium hydroxide (25%) were provided by China National Medicines Co. Ltd. (Shanghai, China).

2.2 Methods

2.2.1 Synthesis of CTS modified sepiolite (CTS-sep)

The CTS-sep with excellent performance can adsorb more AR73 molecules to form hybrid pigment. To optimize the CTS-sep with the maximum dye immobilisation, the AR73 adsorption capacity of the CTS-sep at different dosages of CTS and HAc were studied. The CTS-sep was prepared according to the following steps: Dissolving CTS in 200 mL 1-5% HAc to form solutions with concentrations of 0.5-10 g/L. Then the sepiolite (2.00 g) was dispersed in the CTS solution, mixed with high shear for 6 h.

Then the suspension was centrifuged for 5 minutes at 9000 rmp and dried at 70℃ for 12-24 h.

2.2.2 Synthesis of CTS-sep/AR73 pigment

AR73 (2.5-5.0 mg) was dissolved in 100ml ultrapure water. Then the pH of AR73 solution was adjusted to 2-9 with 0.1 mol/L NaOH and 0.1 mol/L HCl. CTS-sep (0.05 g) was dispersed in 20 ml AR73 solution. And the mixture was magnetically stirred to reach the adsorption equilibrium. After the centrifugtion at 9000 rmp for 5 minutes, the supernatant was removed. The solid was rinsed with distilled water until the supernatant became clear, indicating non-adsorbed AR73 was completely removed. The precipitate was dried at 70℃ for 12-24 h and then ground.

2.2.3 Synthesis of CTS-sep/AR73@SiO_2 pigment

The procedure for preparing CTS-sep/AR73@SiO_2 hybrid pigment is shown in Figure 2. 0.2 g of CTS-sep/AR73 was dispersed in 30ml distilled water. Then CTAB solution (10ml 1g/L) was added in the CTS-sep/AR73 solution and stirred magnetically for 30 minutes. TEOS was dissolved in 10 ml anhydrous ethanol to form TEOS solutions of 0.2-4 g/L, and then the solution was dropped into CTS-sep/AR73 suspension. Meanwhile the ammonium hydroxide (25%) was used to keep the pH to 10-11 [9, 22]. The mixture was magnetically stirred for 24 h, and the suspension was centrifuged for 5 minutes at 9000 rmp. The CTS-sep/AR73@SiO_2 mixture was rinsed to remove any unreacted CTAB and dried at 70℃ for 12-24 h.

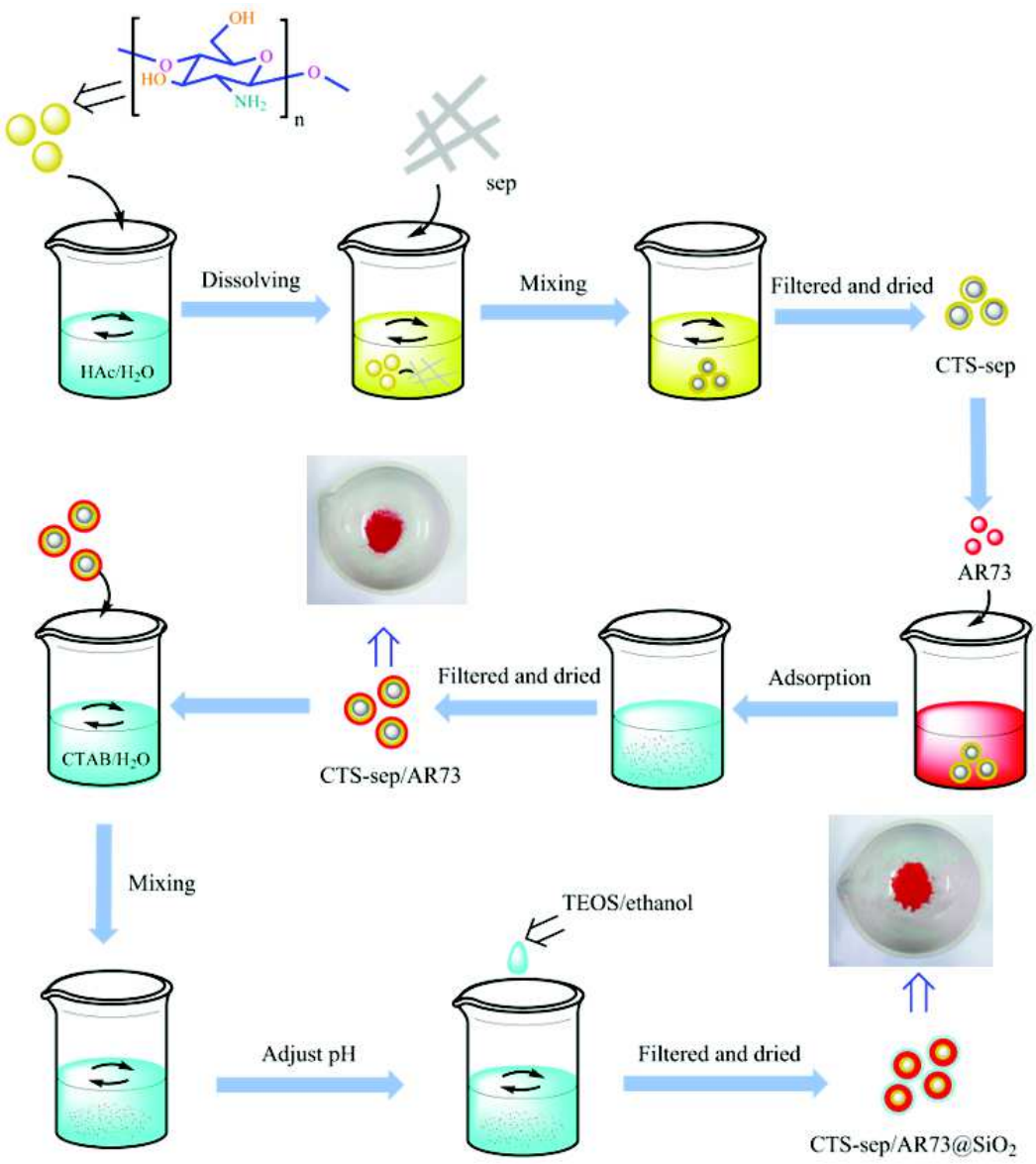

Figure 2. Schematic representation of synthesis steps for CTS-sep/AR73@SiO_2 pigment.

2.2.4 Characterization

The FTIR spectra of AR73, sepiolite, CTS-sep, CTS-sep/AR73, CTS-sep/AR73@SiO_2 were prepared to use KBr pellets in the range of 4000 – 400 cm^{-1} on infrared spectrometer (NICOLET380, USA). The micrographs of sepiolite, CTS-sep, CTS-sep/AR73, CTS-sep/AR73@SiO_2 were obtained by scanning electron microscope (SEM, JSM-6610LV, Japan). UV-Vis spectra of the supernatants were obtained on UV-

Vis spectrophotometer (Agilent Cary 60, USA). The colour change of solution can be recorded by scanning ultraviolet full wavelength, and the concentration of AR73 in solution can be calculated by maximum absorbance at 509 nm. The X-ray diffraction spectra of samples were obtained using an X-ray diffractometer (XRD, D/MAX-2500, Japan) with Cu Kα radiation (40 kV, 40 mA, λ=0.15406 nm), and the scan range was 2θ=5-60°. The zeta potentials of sepiolite, CTS-sep, CTS-sep/AR73, CTS-sep/AR73@SiO_2 were measured using Zetasizer Nanosystem (Zetasizer nano ZS90, UK).

2.2.5 Stability test

The resistance of the pigments to chemical reagents were studied to evaluate the stability of the pigments. 0.02 g simple was dispersed in 20 ml anhydrous ethanol, 1 mol/L NaOH, 1 mol/L HCl respectively, and then the mixtures were magnetically stirred at room temperature for 1d, 2d, 3d. After centrifugation, the supernatant was obtained and analyzed by Uv–Vis spectra. A lower absorbance means less removal of AR73 from the pigment and higher stability of hybrid pigments. In order to study the thermal stability, a thermal analyzer (TGAQ50) was used to analyze samples at a temperature of 30 to 600℃ in a nitrogen atmosphere. The photostability of the AR73, CTS-sep/AR73 and CTS-sep/AR73@SiO_2 hybrid pigments were evaluated employing diffuse-reflectance Uv-Vis spectra.

2.2.6 The removal rate of dye

The adsorption capacity of CTS-sep to AR73 molecules was evaluated by dye removal effieneicy. The removal efficiency was calculated using equation (1):

$$R = \frac{(C_1 - C_2)}{C_1} * 100\% \quad (1)$$

where R is the removal efficiency of dye, c_1 and c_2 represent the concentration of AR73 in the solution before and after adsorption, respectively.

3. Results and discussion

3.1 Preparation of CTS-sep/AR73 pigment

3.1.1 Selection of concentration of AR73 solution in preparation of CTS-sep /AR73 pigment

The UV-Vis spectra of the AR73 aqueous solution after treated by CTS-sep (the concentration of CTS is 0.5 g/L, the concentration of HAc is 1%) are shown in Figure 3, the data of absorbance and concentration before and after AR73 adsorption under different AR73 concentrations are shown in Table 1. It shows that as the initial concentration of the AR73 solution increases, the amount of residual dye in the solution after CTS-sep adsorption increases. When the concentration of AR73 solution is about 70 mg/L, the concentration of AR73 decreased by 35.5118 mg/L and the residual amount of AR73 was too much after adsorbed by 0.05 g CTS-sep, so the maximum adsorption capacity of 20 ml AR73 solution with 0.05 g CTS-sep was about 35 mg/L. At 15 and 5 mg/L, there is too little AR73 remained after adsorption, the absorbance of solution is almost 0, and the maximum adsorption capacity is not reached within these concentration ranges. Therefore, these concentration ranges are not suitable for the adsorption of AR73. It shows that the maximum absorbance in the UV spectrogram reaches 0.1821 Abs when the concentration of AR73 solution is 25 mg/L, the solution is light red after adsorption and the maximum adsorption capacity of CTS-sep can not

be reached. When the concentration of AR73 solution increases to 50 mg/L, the maximum absorbance in the UV spectrogram reaches to 0.5008 Abs and the maximum adsorption capacity of CTS-sep can be reached. When the concentration of AR73 is around 50 mg/L, it can make CTS-sep adsorb enough AR73 and little AR73 remaining after adsorption. Therefore, in the following tests, in order to find which kind of CTS-sep can immobilize more AR73 molecules, the AR73 solution with a concentration around 50 mg/L were selected.

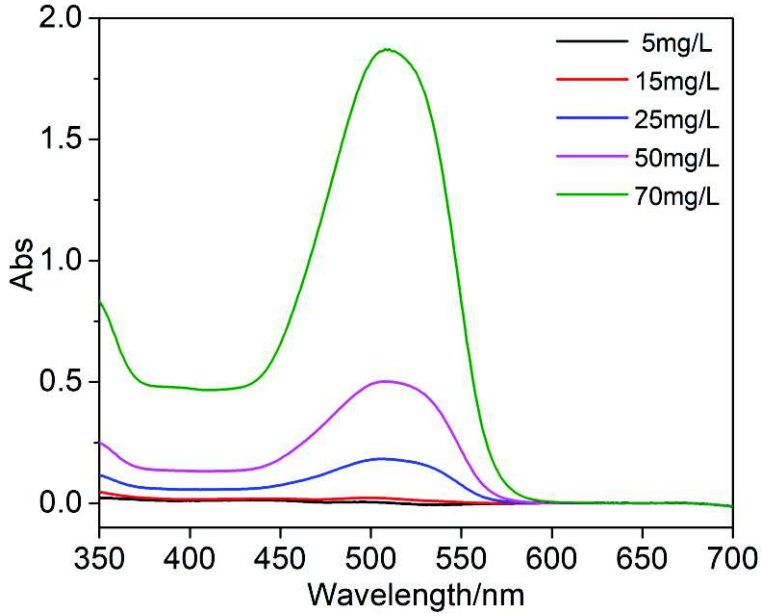

Figure 3. The UV-vis spectra of CTS-sep after adsorption of AR73 with different concentrations.

Table 1 Absorbance and concentration before and after AR73 adsorption under different AR73 concentrations.

Concentration (mg/L)	Maximum Abs (in 509 nm)	The concentration before adsorption(mg/L)	The Abs after adsorption	The concentration after adsorption (mg/L)	Concentration difference (mg/L)
70	3.2493	82.9743	1.8667	47.8205	35.5118
50	1.8841	48.2629	0.5008	13.0913	35.5296
25	1.0964	28.2349	0.1821	4.9880	23.6049
15	0.4704	12.2183	0.0203	0.8741	11.8022
5	0.1706	4.4656	0.0023	0.4165	4.6372

3.1.2 Effect of CTS concentration on preparation of CTS-sep/AR73 pigment

Figure 4a demonstrates the effect of CTS concentration (the concentration of HAc is 1%) on the UV spectra of AR73 in CTS-sep. The UV intensity of AR73 shows the lowest value when CTS is 2.5 g/L in Figure 4a, indicating the maximum AR73 adsorption/removal capacity compared with the other CTS concentrations. Figure 4b displays that the dye removal efficiency increases as the concentration of CTS ranges from 0.5 to 2.5 g /L and then decreases with the amount of CTS increases in the range of 2.5–10 g/L. The highest dye removal efficiency can be observed when the CTS concentration is 2.5±0.1 g/L. The colour change in AR73 solution from dark red to clearly transparent is resulted from the changes in CTS concentration (Figure 4a), reflected in the AR73 UV spectra. Figure 4b also suggests that the ability of CTS-sep to immobilise AR73 increases with the increase of the CTS concentration, and CTS can be more uniformly combined with sepiolite. The viscosity of the solution increase when the CTS concentration increase from 0.5 to 2.5 g/L, which benefits the polymerization of CTS and shows an agglomeration of sepiolite fibers [23]. From 2.5–10 g/L, the sepiolite fibers seem to be tightly bound to CTS and the hardness of CTS-sep increases, these results make it difficult for amino groups on CTS to be protonized, thus reducing the adsorption capacity of AR73 [21].

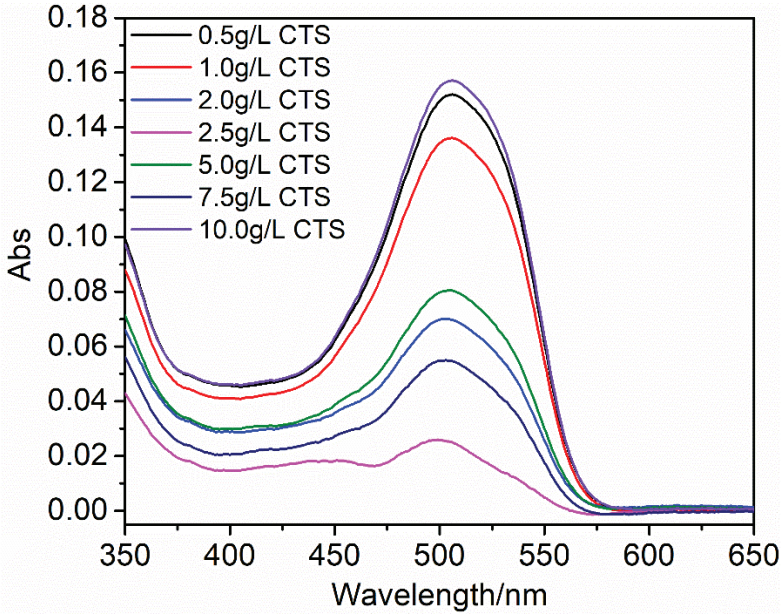

(a)

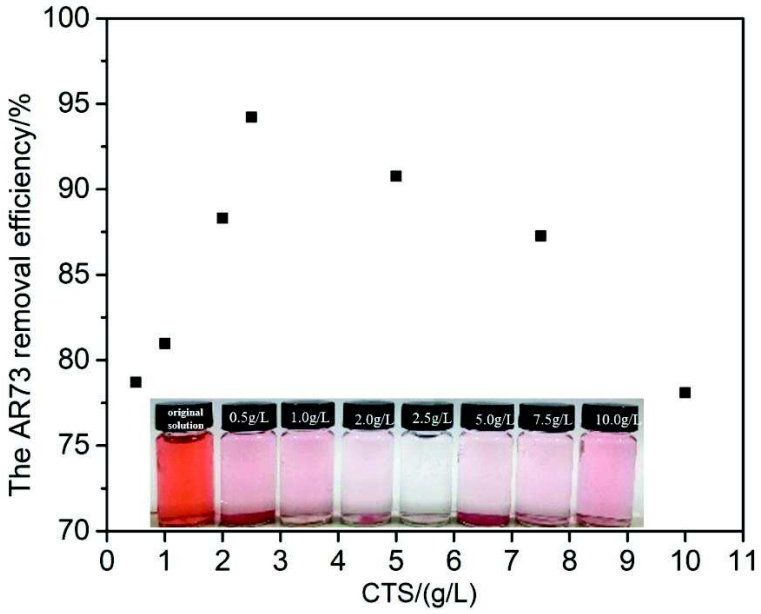

(b)

Figure 4. (a) AR73 UV-Vis spectra of the supernatants at different dosage of CTS, **(b)** the removal efficiency as a function of CTS dosage and the digital images of the supernatants.

3.1.3 Effect of HAc concentration on preparation of CTS-sep/AR73 pigment

The HAc is used to help CTS dissolve in the solvent. The acid group, however, could protonate the CTS amino group [24, 25]. We investigated the effect of the acidity of

HAc on the AR73 adsorption performance in order to find the optimal HAc concentration for the maximum of AR73 adsorption. The AR73 UV spectra of the CTS-sep/AR73 hybrid pigments are presented in Figure 5a. The AR73 UV intensity reaches the lowest point when the concentration of HAc is 2%, indicating that the CTS-sep had the highest AR73 adsorption capacity. And the dye removal efficiency can increase to 95% when the HAc concentration is at 2% in Figure 5b, leading to colour fading of the supernatants. When the concentration of HAc is 2%, the total protonation of amino groups is allowed, and in such case, CTS deposition is more uniform [23]. At lower concentration of HAc, CTS is easy to agglomerate and tends to deposit unevenly, leading to the decrease of CTS-sep adsorption [26]. When the concentration of HAc is in the range of 3-5%, the viscosity of CTS increases with increasing concenteration [27]. Excessive concentration of HAc will lead to irregular volume shrinkage of CTS, which could not uniformly cover the surface of sepiolite, thus reducing the ability of CTS-sep to absorb AR73. According to the effects of CTS concentration and HAc concentration on AR73 adsorption capacity, the optimal concentrations of CTS and HAc are determined, which are 2.5 g/L for CTS and 2% for HAc, respectively.

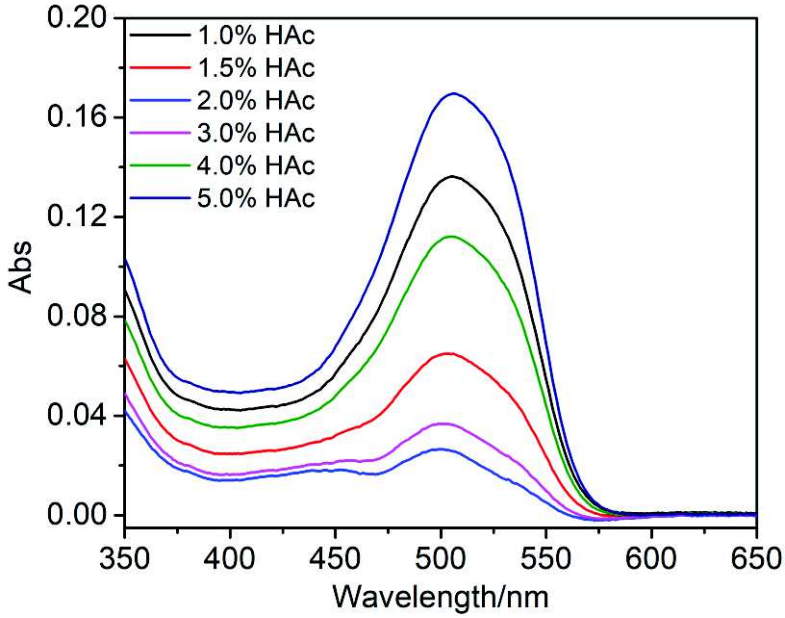

(a)

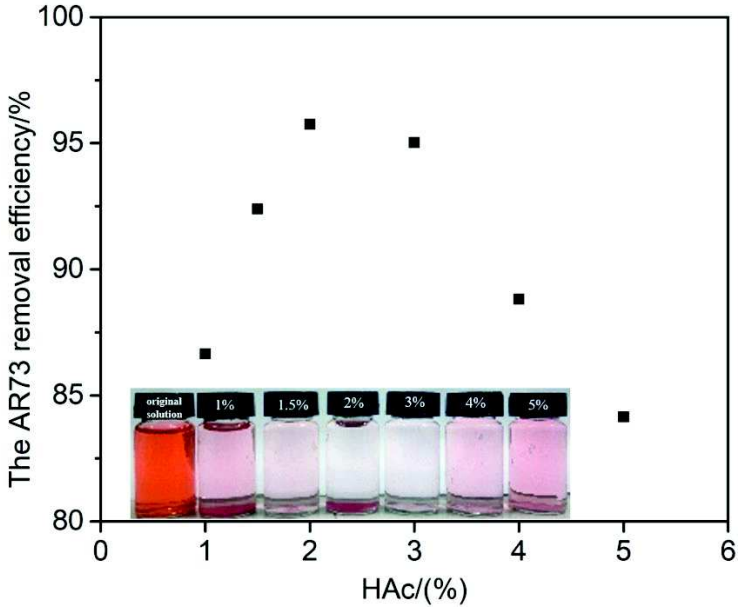

(b)

Figure 5. (a) AR73 UV-Vis spectra of the supernatants after mixing with modified sepiolite at different HAc concentrations, **(b)** the AR73 removal efficiency the supernatants photos.

3.1.4 Effect of adsorption time on the preparation of CTS-sep/AR73 pigment

Adsorption time is also one of the factors that affect the formation of CTS-sep/AR73 pigment. In order to explore the adsorption equilibrium time of AR73, the relationship

between adsorption time and AR73 removal efficiency was studied. As can be seen from Figure 6, the dye removal efficiency increased rapidly within 60 minutes and reached a maximum value within 60 minutes, at this time the removal efficiency was 91.79. Then, with the increase of time, the dye removal efficiency is around 91% and tends to balance. It can be seen from the digital photos of the AR73 solution after different adsorption times in the Figure 6. The color of the AR73 solution becomes lighter with the increase of adsorption time. After the adsorption time reaches 60 min, the color of the solution hardly changes. Therefore, according to the relationship between the adsorption time and the removal efficiency of AR73, the time reach adsorption equilibrium was determined to be 60 minutes.

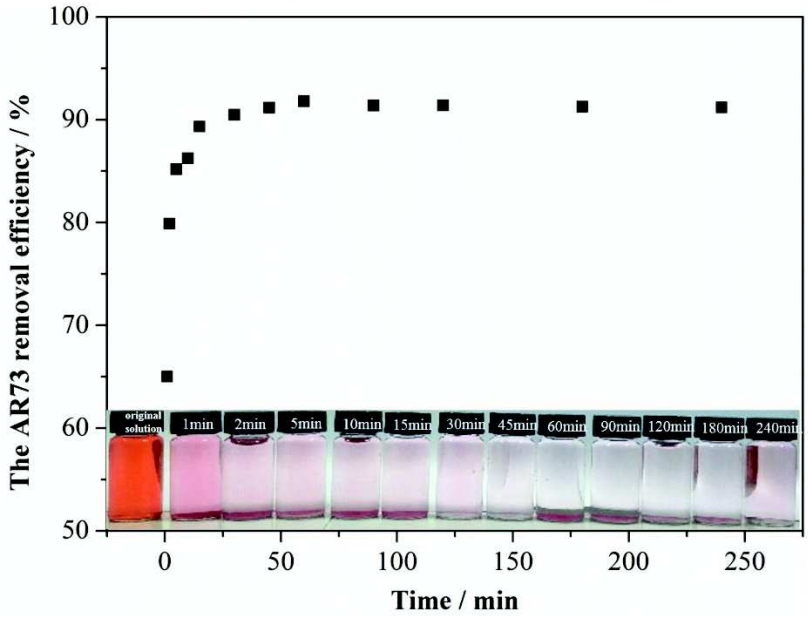

Figure 6. Removal efficiency of AR73 varies with adsorption time.

3.1.5 Effect of pH value of AR73 solution on preparation of CTS-sep/AR73 pigment

In the preparation of CTS-sep/AR73, the dye removal efficiency in AR73 solutions

with different pH values is displayed in Figure 7. The dye removal rate increases first and then decreases with the pH ranges from 2 to 9. This result indicates that the adsorbent CTS-sep is able to remove AR73 in a wide range of pH (2-9). The highest dye removal efficiency is achieved at the pH of 5, and the dye removal efficiency decreases abruptly when the pH value is 9. The reason for this phenomenon is resulted from the protonation of amine groups in CTS before AR73 adsorption under acidic conditions. In aqueous solution, the AR73 (acid dye) are first dissolved and the sulfonate groups of AR73 (D-SO_3Na) are dissociated and converted to anionic dye ions [24]. Also, in the presence of H^+, the amino groups of the CTS (R-NH_2) became protonated. At low pH (less than 5), the amount of AR73 interacting with the active site of CTS-sep may decrease due to the reduction of dye dissociation. The azo groups in AR73 molecules are unstable and prone to dissociation under strong acidic conditions. Our investigation has a good agreement with other research groups on the optimum pH of pH 3-6 for AR73 removal by CTS [28]. From pH=5, as the pH of the AR73 solution increases, the amount of dye adsorption decreases. The decrease of AR73 adsorption at high pH is due to the decrease of protonated NH_2 group, and a large number of OH^- ions in the solution compete with the adsorption sites of AR73 anions, therefore the adsorption capacity for the AR73 decrease at high pH [24, 29].

To sum up, so as to achieve the maximum AR73 adsorption by the CTS-sep, the optimal preparation conditions to form CTS-sep/AR73 hybrid pigment are 2.5 g/L for CTS, 2 % for HAc and at pH=5.

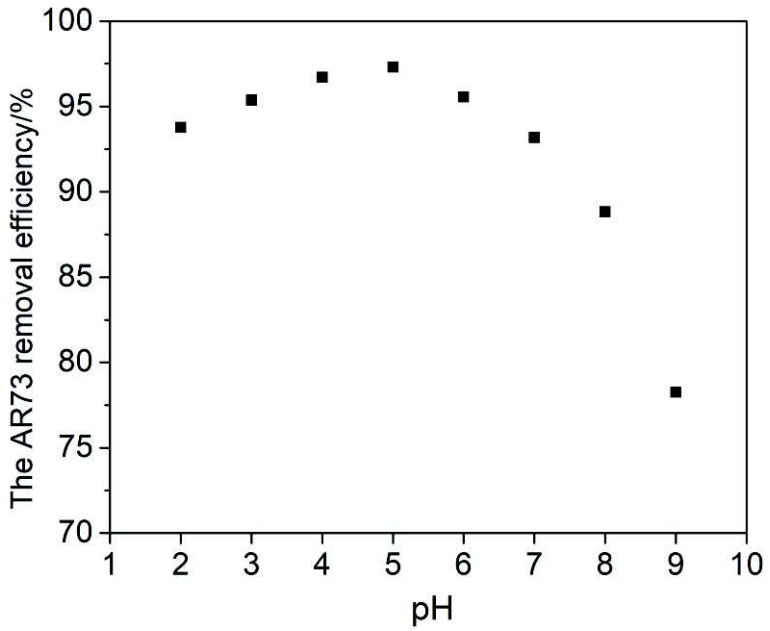

Figure 7. The AR73 removal efficiency as a function of different pH values.

3.2 Preparation of CTS-sep/AR73@SiO_2 pigment

On the surface of CTS-sep/AR73 pigment, the layer of SiO_2 was used which was obtained by hydrolysis and condensation of TEOS at room temperature to enhance the stability of CTS-sep/AR73 pigment [30, 31]. CTAB, as a cationic surfactant is employed to increase the surface potential of CTS-sep/AR73, and the negatively charged silica is greatly beneficial to the coating by electrostatic action [9]. The introduction of CTAB improves the homogeneity of dispersed hybrid pigment particles, which is beneficial to silica coating [9, 31, 32]. From Figure 8, the colour of the supernatant after 1-2 d of exposure in anhydrous ethanol shows the lightest colour as the concentration of TEOS is 2.0 g/L, so the intensity of the absorption peak is the lowest at this concentration. The lower absorbance of the supernatant, the higher stability of the pigment against elution [30]. The UV intensity of CTS-sep/AR73 (orange curves) without SiO_2 layer in Figure 8. is the highest, which indicates that

AR73 is desorbed from CTS-sep/AR73 into the ethanol solvent. The result demonstrates that the stability of the CTS-sep/AR73@SiO_2 pigment in ethanol has been improved owing to the protection of SiO_2 layer onto AR73 molecules. Furthermore, Figure 8. also shows that the stability of CTS-sep/AR73@SiO_2 pigment decrease when the dosage of TEOS over 2 g/L. This is due to the fact that excessive TEOS impede the hydrolysis of TEOS to SiO_2 [33]. Therefore, the optimal concentration of TEOS to form stable CTS-sep/AR73@SiO_2 pigment is 2.0 g/L.

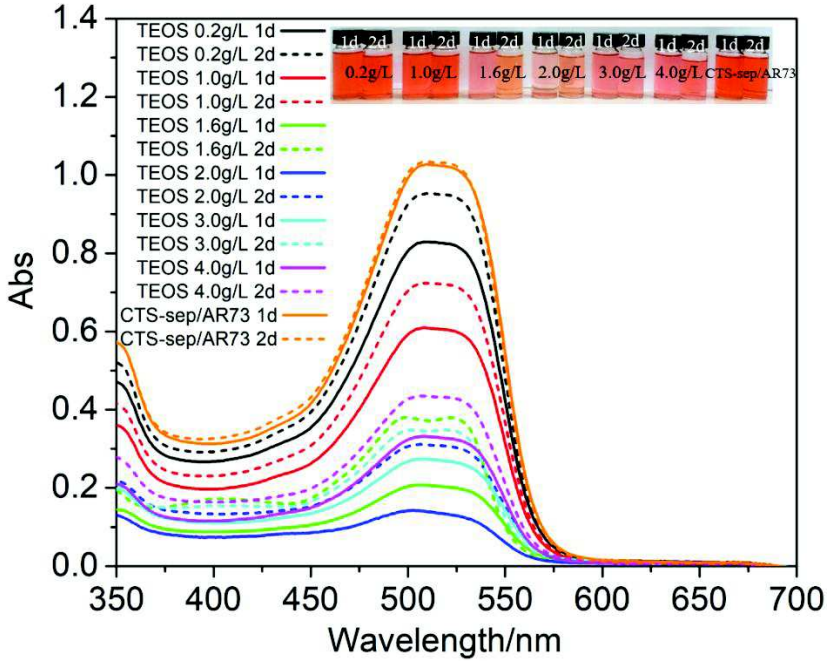

Figure 8. AR73 UV-Vis spectra of the supernatants of CTS-sep/AR73@SiO_2 at different dosages of TEOS after ecposure of ethanol for 1-2d. The inset photos are the supernatants of CTS-sep/AR73@SiO_2 and CTS-sep/AR73 without SiO_2 layer.

3.3 Structural characterisation of CTS-sep/AR73 and CTS-sep/AR73@SiO_2 pigments

The samples used to characterization was prepared under the following conditions. The CTS-sep/AR73 hybrid pigment was obtained by adsorbing CTS-sep in AR73

solution at pH=5. CTS-sep/AR73@SiO_2 hybrid pigment was prepared by the modification of CTS-sep/AR73 hybrid pigment in CTAB solution at pH=1 and the TEOS concentration of 2.0 g/L.

The surface morphologies of CTS-sep/AR73 and CTS-sep/AR73@SiO_2 hybrid pigments are shown in Figure 9. The rod-like crystals of sepiolite (Figure 9a) are developed and tightly packed together [34]. The surface of sepiolite (Figure 9b) crystals are smooth and the fibers of sepiolite are flat or straight [17, 35]. CTS-sep in Figure 9c shows a disaggregate fiber morphology and the nanofibers are broken into smaller fibers due to the long magnetic stirring. Figure 9c shows the agglomeration of sepiolite fibers after CTS modification [21]. This is because the amine groups of CTS could combine the siloxane (Si-O-Si), hydroxyl (Mg-OH) of sepiolite by hydrogen-bond [23, 36]. For CTS-sep/AR73 hybrid pigment (Figure 9d), due to the adsorption of AR73, the surface of CTS-sep/AR73 become rougher, the crystal bundles become shorter. These indicate the successful binding of AR73 onto CTS-sep. The size of CTS-sep/AR73@SiO_2 (Figure 9e) is slightly thicker than that of CTS-sep/AR73 without SiO_2. CTS-sep/AR73@SiO_2 (Figure 9f) has a smoother surface due to a thin layer of amorphous SiO_2.

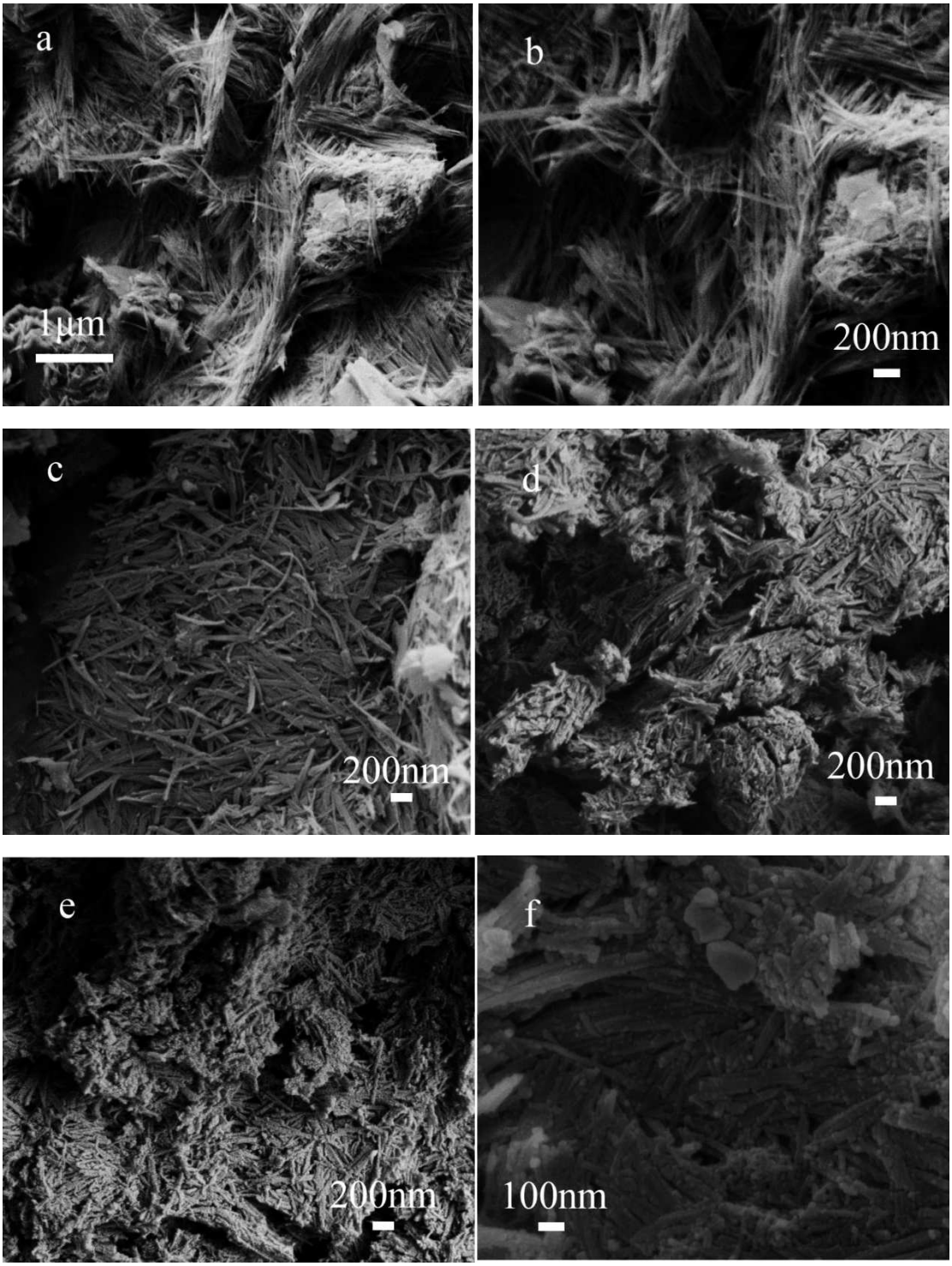

Figure 9. SEM images of **(a, b)** sepiolite, **(c)** CTS-sep, **(d)** CTS-sep/AR73 and **(e, f)** CTS-sep/AR73@SiO_2.

The XRD spectras of sepiolite, CTS-sep, CTS-sep/AR73, and CTS-sep/AR73@SiO_2 pigments are shown in Figure 10. The XRD spectra of the sepiolite (in Figure10a)

shows the diffraction peaks of sepiolite ($Mg_8Si_{12}O_{30}(OH)_4(OH_2)_{4n}H_2O$), calcite ($CaCO_3$), quartz ($SiO_2$) [37]. Compared with the peaks of sepiolite, the characteristic peaks of CTS-sep have obvious difference, the intensity of peaks assign to calcite (2θ at 29.3, 30.8) vanished. This is due to the decomposition of calcite in the sepiolite for the acidic CTS solution. The other peaks display in Figure 10b mean that the sepiolite structures are preserved after the CTS modification [35]. There is no significant change in the structure of CTS-sep/AR73 compared with CTS-sep, which indicates that the crystal structure of CTS-sep hasn't been destroyed and the AR73 molecules are adsorbed on the grooves, the outer surface and the openings of the channels of CTS-sep, but cannot enter the channels [11]. The peaks of CTS-sep/AR73@SiO_2 have no obvious changes, but the peak strength of CTS-sep/AR73@SiO_2 is not high as that of CTS-sep/AR73, which may be due to the coating of SiO_2 on the material [6, 38].

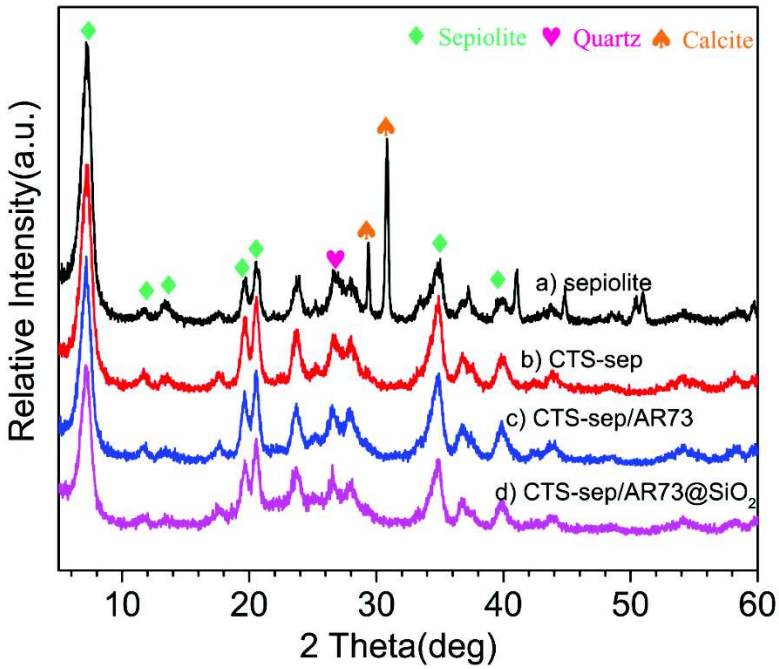

Figure 10. XRD patterns of sepiolite, CTS-sep, CTS-sep/AR73, and CTS-sep/AR73@SiO_2.

The zeta potentials of sepiolite, CTS-sep, CTS-sep/AR73, and CTS-

sep/AR73@SiO_2 are shown in Table 2. Sepiolite illustrates a zeta potential of -11.5 mv, which is similar to the published data [11]. CTS contains a lot of hydroxyl groups and amino groups [18]. The amino group in the CTS structure can be protonated by a small amount of acidic solution. Then the polysaccharide can be used as a polymeric electrolyte to compensate for the negatively charged sepiolite. Besides, hydrogen bonds can also be formed between the hydroxyl group of CTS and the silanol group of sepiolite [21]. Therefore, the surface potential of CTS-sep is significantly increased to 8.4 mv, as shown in Table 2. The zeta potential of CTS-sep/AR73 is 4.35 mv. AR73 is the anionic dye whose solid surface potential presents a negative charge. Therefore, the AR73 molecules can be adsorbed on CTS-sep via electrostatic interaction. Consequently, compared with CTS-sep, the surface potential of CTS-sep/AR73 decreased due to the adsorption of AR73 molecules. The zeta potential significantly decreases to -4.74 mv after introducing the negative charged SiO_2 layer at pH=3-11[39]. The surface potential changes of CTS-sep/AR73 and CTS-sep/AR73@SiO_2 also prove that the modification of the CTS-sep/AR73 pigment by TEOS polycondensation is successful.

Table 2. Zeta potentials data of sepiolite, CTS-sep, CTS-sep/AR73, and CTS-sep/AR73@SiO2 hybrid pigments.

Sample	sepiolite	CTS-sep	CTS-sep/AR73	CTS-sep/AR73@SiO_2
Zeta potentials (mv)	-11.50	8.40	4.35	-4.74

FTIR spectra of sepiolite, AR73, CTS, CTS-sep, CTS-sep/AR73, CTS-sep/AR73@SiO_2, CTAB and TEOS are shown in Figure 11. The broad intensity band

at 3416 cm^{-1} in the sepiolite spectrum (Figure 11a) is the H-O-H vibrations of adsorbed water in the sepiolite, while the broad intensity at 1636 cm^{-1} is caused by the deformation of OH group of water [11]. The band at 1447 cm^{-1} is the CO vibration and 880 cm^{-1} is the symmetric deformation of $-CO_3^-$ [15, 40]. In the AR73 spectrum (Figure 11b), both of the strong absorption bands at 1632 and 1448 cm^{-1} correspond to the skeletal vibration of phenyl groups, while the bands at 1207 and 1036 cm^{-1} belong to the antisymmetric and symmetric stretching vibration of $-SO_3^-$ groups, respectively [4, 41]. Many bands between 900 and 700 cm^{-1} are caused by the aromatic out-of-plane C-H vibrations and ring out-of-plane vibrations. The absorption band at about 700 cm^{-1} provides evidence for mono-substituted benzene rings [42].

Comparing the FTIR spectra of CTS-sep, sepiolite and CTS (Figure 11d, Figure 11a and Figure 11c), it can be found that the band of CTS-sep disappeared at 1447 cm^{-1} for C=O vibration, while the stretching vibration peak of C–N band of CTS appeared at 1384 cm^{-1} [43]. Compared with sepiolite, the intensity of the silanol band around 3500 cm^{-1} in CTS-sep is reduced due to the coverage of CTS on the surface of sepiolite [21, 44]. The spectrum of CTS-sep/AR73 showes that the $-SO_3-$ group of AR73 has symmetric stretching vibration at 1207cm^{-1}, and the monosubstituted benzene ring of AR73 appeares near 700cm^{-1} [45, 46]. Therefore, it can be proved that AR73 molecule has been adsorbed on the surface of CTS-sep. The Si–O–Si asymmetric stretching vibration band of 980–1190 cm^{-1} is found in CTS-sep/AR73@SiO_2 [22, 47]. The TEOS (Figure 11h) shows three absorption bands: at around 1090, 805 and 470 cm^{-1} [48], these three absorption bands can also be found in CTS-sep/AR73@SiO_2 spectra.

Compared with TEOS spectra, the free silanol hydroxyl group (Si-OH) disappeared at 960 cm^{-1} in CTS-sep/AR73@SiO_2 spectra [22]. In addition, -CH_3 and -CH_2- appear at 2927 and 2858 cm^{-1}, proving the existence of CTAB [9]. These can be proved that SiO_2 was successfully coated on CTS-sep/AR73 hybrid pigment.

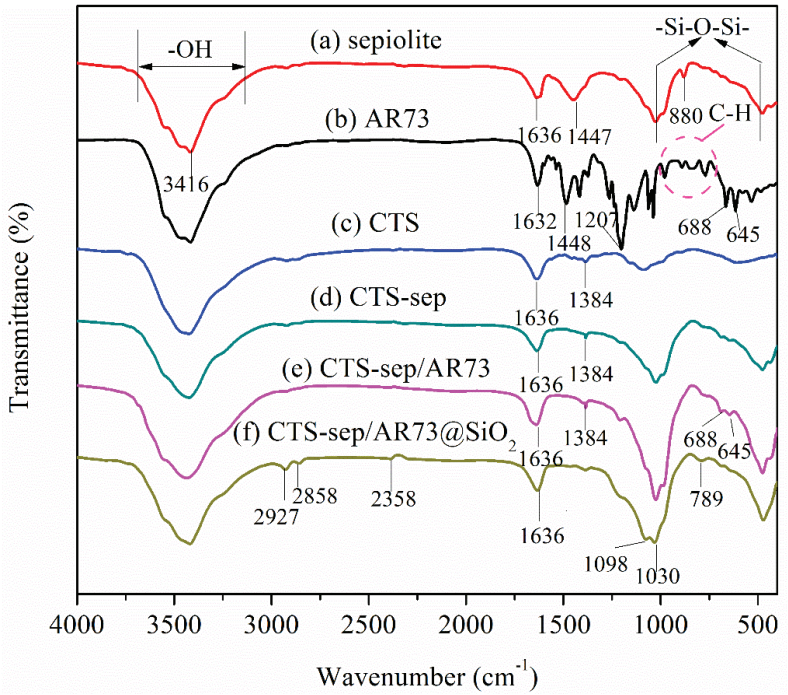

(a)

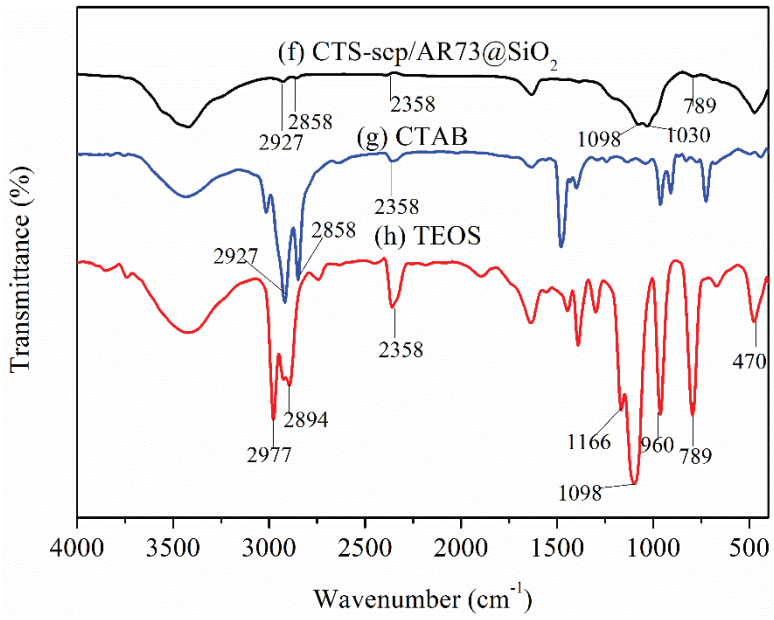

(b)

Figure 11. FTIR spectra of sepiolite, AR73, CTS-sep, CTS-sep/AR73, CTS-sep/AR73@SiO_2.

A proposed mechanism for CTS-sep/AR73 hybrid pigment formation is shown in Figure 12 (a). CTS is dissolved in HAc solution initially, followed by the protonation of amino group in the CTS structure under slightly acidic condition. In this protonation, the polysaccharide acts as a polyelectrolyte to compensate for the negatively charged sepiolite [21]. In addition, on the external surface of the sepiolite, hydrogen bonds can also be formed between the hydroxyl group of the CTS and the silanol group [21, 49]. When the CTS-sep/AR73 hybrid pigment is formed, the pH of the AR73 solution is adjusted to 5. There are sulfonic acid groups in the molecule of AR73. These sulfonic acid groups exist in the form of negative ions in weakly acidic solutions. The amino groups on chitosan can be protonated in weakly acidic solutions. The protonated amino group and sulfonic acid group immobilize the AR73 molecule on the CTS-sep through electrostatic interaction [50]. The AR73 molecule forms a hydrogen bond with the hydroxyl group of the CTS and then form an electrostatic interaction with the amino positive ion so that the molecule can be stably immobilized on the modified sepiolite. A proposed mechanism for CTS-sep/AR73SiO_2 hybrid pigment formation is shown in Figure 12 (b). It is mainly attributed to electrostatic interaction. After SiO_2 is coated, CTAB is used to enhance the surface potential of the CTS-sep/AR73 pigment to form an electrostatic interaction with the negative potential of the SiO_2. CTAB can play the role of coupling agent in CTS-sep/AR73 pigment suspension, which facilitates the formation of the SiO_2 layer on the surface of the CTS-sep/AR73 pigment by TEOS [9, 22].

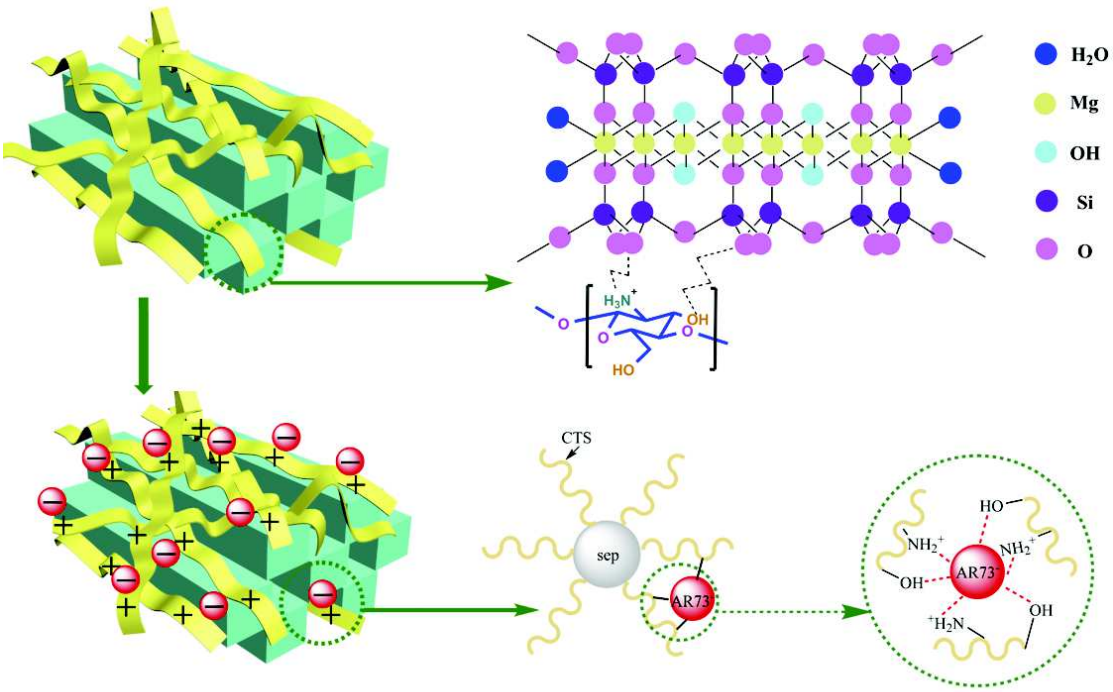

(a)

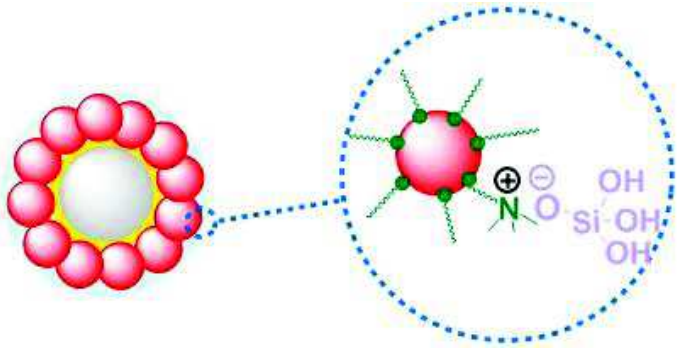

(b)

Figure 12. (a), Mechanism of sepiolite modification and adsorption of AR73 by CTS-sep, (b), Mechanism of CTS-sep/AR73@SiO_2.

3.4 Stability of CTS-sep/AR73 and CTS-sep/AR73@SiO_2 pigment

The thermal stability of CTS-sep/AR73@SiO_2 and CTS-sep/AR73 pigments were evaluated by TGA and DTG. As shown in the Figure 13, comparing CTS-sep/AR73@SiO_2, CTS-sep/AR73 and CTS-sep in Figure 13, the weight loss of CTS-

sep/AR73@SiO_2 and CTS-sep/AR73 is obviously less than that of CTS-sep in all range. That means that thermal stability of CTS-sep/AR73@SiO_2 and CTS-sep/AR73 is higher than that of CTS-sep. As can be seen from the DTG curve of AR73 in Figure 13b, the significant exothermic peaks of AR73 at 120 and 280℃ demonstrate decomposition at these temperatures. From the DTG curves of sepiolite, CTS-sep and CTS-sep/AR73, it can be seen that the exothermic peak at 200-300℃ of CTS-sep/AR73 moves to a higher temperature than that of sepiolite and CTS-sep, indicating that the thermal stability of CTS-sep/AR73 is greater than that of sepiolite and CTS-sep. There is no obvious change of the CTS-sep/AR73@SiO_2 DTG curve at 200-300℃, which shows that CTS-sep/AR73@SiO_2 has a higher themal stability than that of AR73 and the CTS-sep/AR73. All the results show that the thermal stability of AR73 is improved after forming a composite with CTS-sep and modifying its surface with SiO_2. This is due to the host-guest interaction between AR73 and CTS-sep, and the shielding effect of SiO_2.

Samples of CTS-sep/AR73@SiO_2 and CTS-sep/AR73 hybrid pigments were heated at 220℃ for 2 h. And the digital images of the resulting solids and original solids are shown in Figure 14. When the samples were heated at 220℃, CTS-sep/AR73 hybrid pigment turned black (Figure 14c), while the color of CTS-sep/AR73@SiO_2 had no significant changes. This indicated that CTS-sep/AR73@SiO_2 hybrid pigment is more stable at higher temperature than CTS-sep/AR73 hybrid pigment.

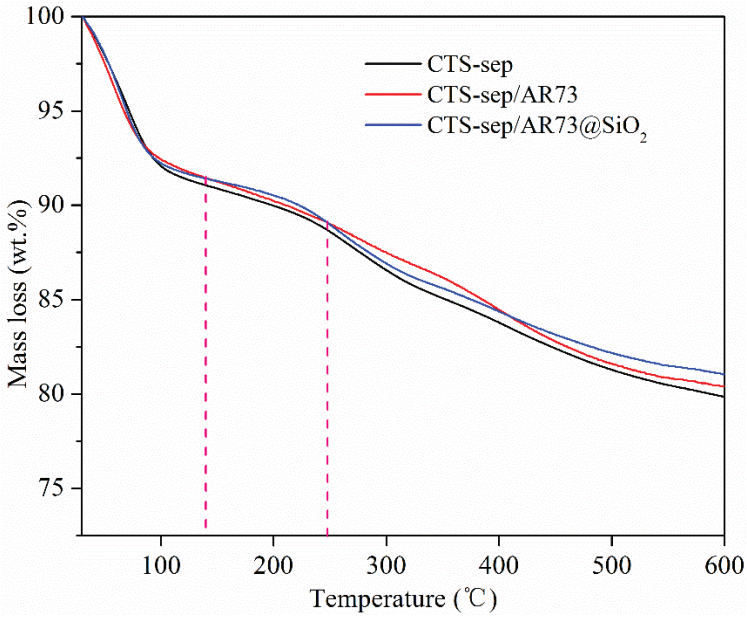

(a)

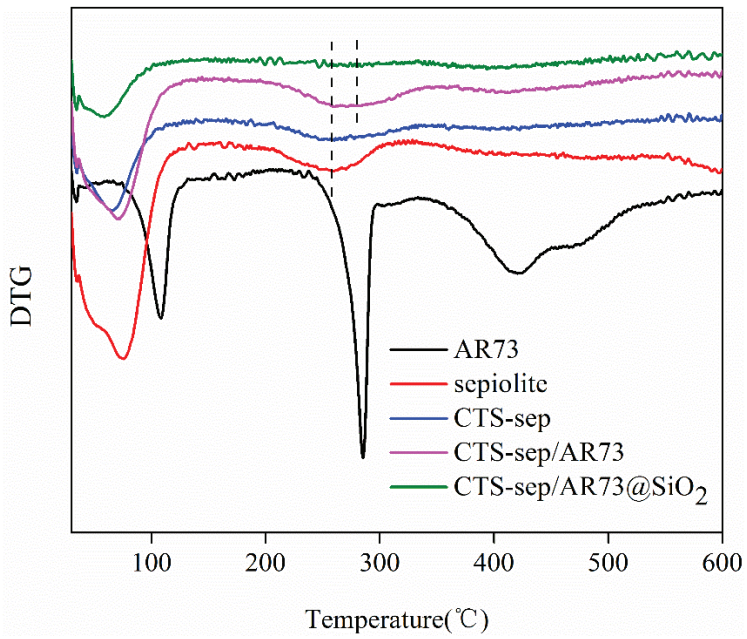

(b)

Figure 13. TGA and DTG curves of AR73, CTS-sep, CTS-sep/AR73, and CTS-sep/AR73@SiO_2 pigments in N_2 atmosphere.

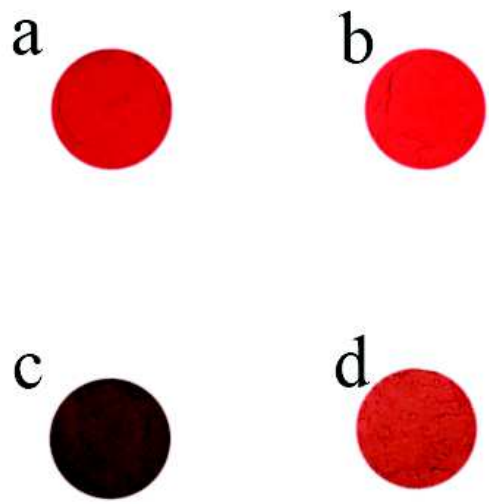

Figure 14. Photos of **(a)** CTS-sep/AR73 hybrid pigment at room temperature **(b)** CTS-sep/AR73@SiO_2 hybrid pigment at room temperaure **(c)** CTS-sep/AR73 hybrid pigment heated at 220℃ **(d)** CTS-sep/AR73@SiO_2 hybrid pigment heated at 220℃.

To evaluate the chemical stability of the CTS-sep/AR73 and CTS-sep/AR73@SiO_2 hybrid pigments, the pigments are immersed in anhydrous ethanol, 1M NaOH and 1M HCl at room temperature for 1-3 days, and the reeults are presented in Figure 15. From Figure 15a, an obviously color difference can be seen between CTS-sep/AR73 and CTS-sep/AR73@SiO_2 hybrid pigment supernatant after treated by 1M HCl, demonstrating that the CTS-sep/AR73 has a lower stability compared with CTS-sep/AR73@SiO_2. The significant difference of the height of the peak on the UV spectrum further confirmed the above conclusion. In Figure 15b, the same trends of the supernatants are observed when exposed to alkaline solution. In Figure 15c, the maximum UV absorbance of the pigment after coating is less than that of CTS-sep/AR73 pigment. Therefore, CTS-sep/AR73@SiO_2 hybrid pigment has demonstrated

a higher stability against acid, alkali, and alcohol than that of the CTS-sep/AR73 hybrid pigment.

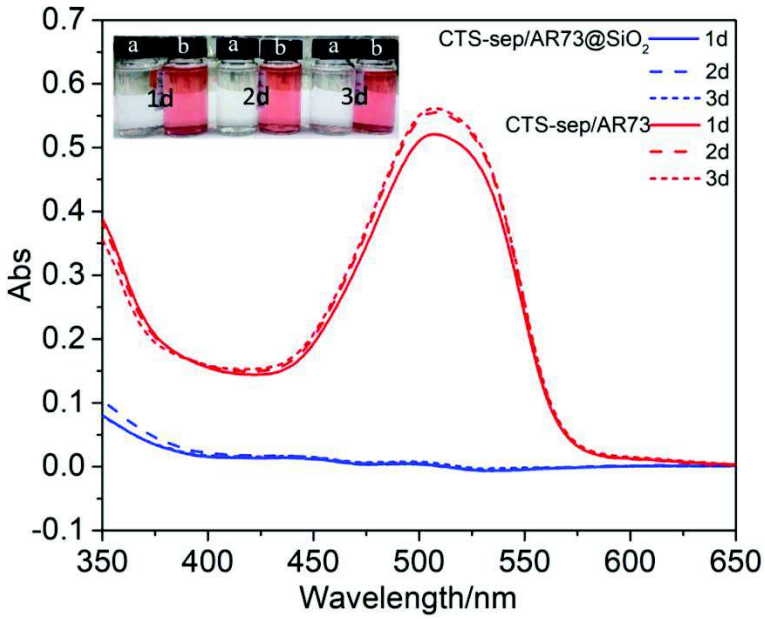

(a)

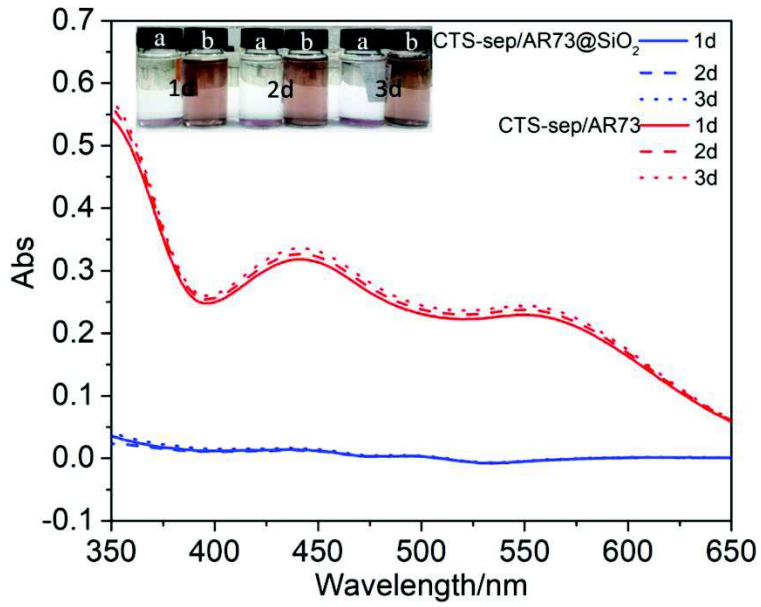

(b)

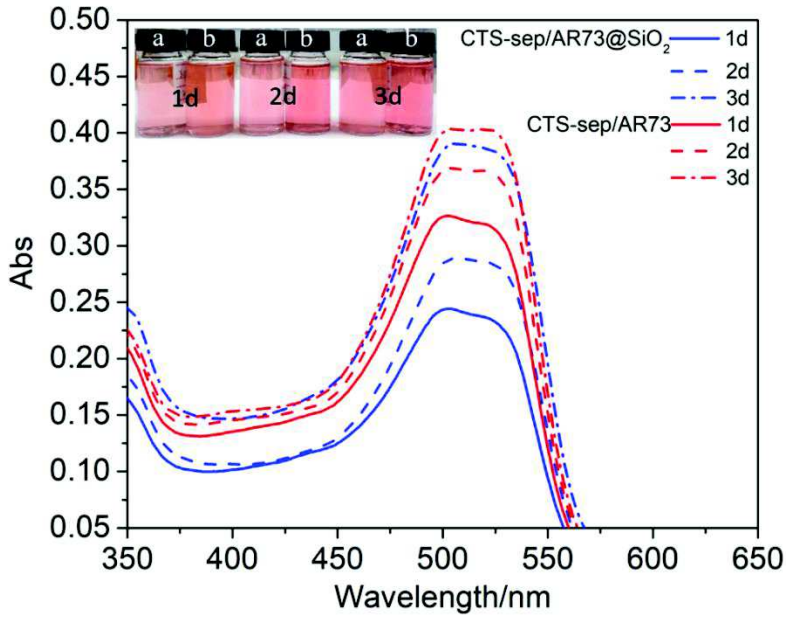

(c)

Figure 15. Variations of UV-Vis spectra and images of the supernatants of CTS-sep/AR73 (a in the photos) and CTS-sep/AR73@SiO_2 (b in the photos) hybrid pigments after chemical exposes of **(a)** 1 M HCl, **(b)** 1 M NaOH and **(c)** ethanol for 3 days.

The photostability of the AR73, CTS-sep/AR73 and CTS-sep/AR73@SiO_2 hybrid pigments were evaluated by diffuse-reflectance Uv-Vis spectra as shown in Figure 16. In diffuse reflectance mode, the spectrum is determined in powder state, therefore, the spectra can be used to characterize the scattering and absorption characteristics of the pigment [7]. The lower the diffuse-reflectance and absorbance of the pigment, the better the scattering performance and the lower photostability of the pigment [16]. In Figure 16, the reflection peak intensity of CTS-sep/AR73 and CTS-sep/AR73@SiO_2 hybrid pigments in the wavelength range of 200-650 nm are significantly stronger than that of AR73, indicating that hybrid pigments can obviously scatter the ultraviolet rays and the hybrid pigment coated with SiO_2 has a better photostability because the strongest

reflectance peaks in Figure 16.

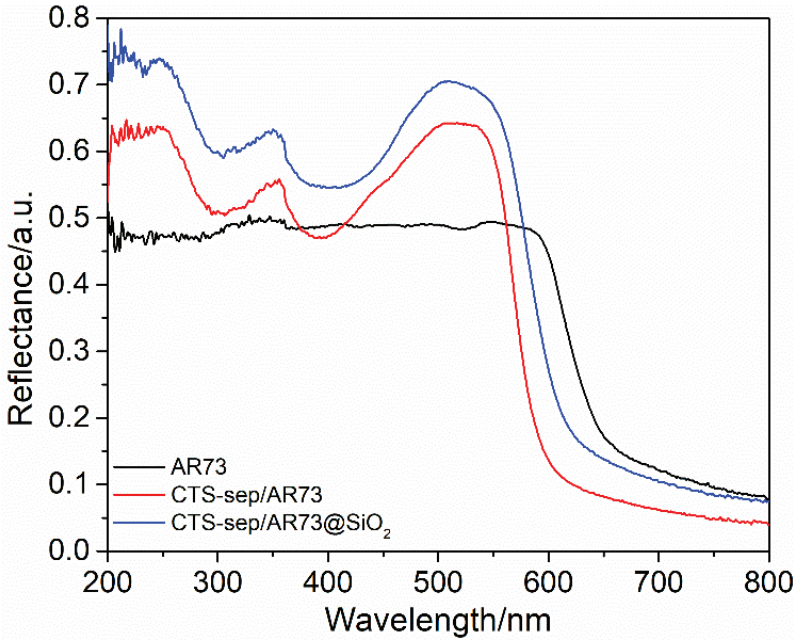

Figure 16. Diffuse-reflectance UV-vis spectra of AR73, CTS-sep/AR73 and CTS-sep/AR73 @SiO_2 hybrid pigments.

4. Conclusions

In this work, we explored the encapsulation of the unstable dye in porous silica to prepare a stable hybrid pigment to widen its applications. Sepiolite was added into CTS solution to prepare CTS-sep as the CTS concentration was 0.5 g/L and the HAc concentration was 2%. AR73 molecule was adsorbed by CTS-sep at pH=5 to obtain the CTS-sep/AR73 hybrid pigment. In this optimal condition, the maximum AR73 adsorption capacity on the CTS-sep/AR73 can be achieved. Consequently, the solubility can be significantly reduced, leading to wide applications of organic dyes. AR73 molecules are immobilized on the CTS-sep by electrostatic interaction and hydrogen bonding. In order to improve the stability of the pigment, 2 g/L TEOS was used as the raw material and ammonia was used as as the catalyst to coat SiO_2 on CTS-

sep/AR73 to form CTS-sep/AR73@SiO_2. Not only does CTS-sep/AR73@SiO_2 pigment has excellent chemical stability against ethanol, 0.1 M NaOH and 0.1 M HCl, but alos excellent thermal stability and intensive UV resistance, which can stay stable at 220℃.

5. Acknowledgements

The authors acknowledge the National Natural Science Foundation of China (21506181, 21506179, 51608464), Hunan province science and technology department (2019JJ30022, 2019SK2112, 2019JJ40281, 2018RS3088, 2018SK2027, 2017TP2026, 2017JJ3291, 2020JJ5534), Guangdong Basic and Applied Basic Research Foundation (2019A1515110919). Research Centre of Chemical Process Simulation Engineering for National Department of Education, Hunan Key Laboratory of Chemical Process Integration Technology for Friendly Environment, National & Local United Engineering Research Centre of Chemical Process Simulation and Intensification, Optimization and Collaborative Innovation Center of New Chemical Technologies for Environmental Benignity and Efficient Resource Utilization and Xiangtan science and technology project. Hunan Provincal Engineering Research Center of Sepiolite Resource for Efficient Utilization.

References

[1] Chen T, Tang P, Feng Y, Li D. Facile Color Tuning, Characterization, and Application of Acid Green25 and Acid Yellow25 Co-intercalated Layered Double Hydroxides. Industrial & Engineering Chemistry Research. 2017;56(19):5495-504. https://doi.org/10.1021/acs.iecr.7b00279.

[2] Chakraborty C, Dana K, Malik S. Intercalation of Perylenediimide Dye into LDH Clays: Enhancement of Photostability. The Journal of Physical Chemistry C. 2010;115(5):1996-2004. https://pubs.acs.org/doi/10.1021/jp110486r.

[3] Tang P, Deng F, Feng Y, Li D. Mordant Yellow 3 Anions Intercalated Layered Double Hydroxides: Preparation, Thermo- and Photostability. Industrial & Engineering Chemistry Research. 2012;51(32):10542-5. https://doi.org/ 10.1021/ie300645b.

[4] Yang L, Qian L, Feng Y, Tang P, Li D. Acid Blue 129 and Salicylate Cointercalated Layered Double Hydroxides: Assembly, Characterization, and Photostability. Industrial & Engineering Chemistry Research. 2014;53(46):17961-7. https://doi.org/ 10.1021/ie502893f.

[5] Muthukumar M. Studies on the effect of inorganic salts on decolouration of acid dye effluents by ozonation. Dyes and Pigments. 2004;62(3):221-8. https://doi.org/10.1016/j.dyepig.2003.11.002.

[6] Cao L, Fei X, Zhao H, Gu Y. Inorganic–organic hybrid pigment fabricated in the preparation process of organic pigment: Preparation and characterization. Dyes and Pigments. 2015;119:75-83. https://doi.org/ 10.1016/j.dyepig.2015.03.020.

[7] Junjie Y, Shuxue Z, Limin W, Bo Y. Organic pigment particles coated with titania via sol-gel process. Journal of Physical Chemistry B. 2006;110(1):388-94. https://doi.org/10.1021/jp053938t.

[8] Yuan J, Xing W, Gu G, Wu L. The properties of organic pigment encapsulated with nano-silica via layer-by-layer assembly technique. Dyes & Pigments. 2008;76(2):463-9. https://doi.org/10.1016/j.dyepig.2006.10.002.

[9] Zhang Y, Zhang J, Wang A. Facile preparation of stable palygorskite/methyl violet@SiO_2 "Maya Violet" pigment. Journal of colloid and interface science. 2015;457:254-63. https://doi.org/ 10.1016/j.jcis.2015.07.030.

[10] Zhao X, Li J, Liu Y, Zhang Y, Qu J, Qi T. Preparation and mechanism of TiO_2-coated illite composite pigments. Dyes and Pigments. 2014;108:84-92. https://doi.org/10.1016/j.dyepig.2014.04.022.

[11] Wu S, Duan Z, Hao F, Xiong S, Xiong W, Lv Y, et al. Preparation of acid-activated sepiolite/Rhodamine B@SiO_2 hybrid fluorescent pigments with high stability. Dyes and Pigments. 2017;137:395-402. http://dx.doi.org/10.1016/j.dyepig.2016.10.030.

[12] Zhang Y, Wang W, Zhang J, Liu P, Wang A. A comparative study about adsorption of natural palygorskite for methylene blue. Chemical Engineering Journal. 2015;262:390-8. https://doi.org/ 10.1016/j.cej.2014.10.009.

[13] Jesionowski T, Pokora M, Tylus W, Dec A, Krysztafkiewicz A. Effect of N-2-(aminoethyl)-3-aminopropyltrimethoxysilane surface modification and C.I. Acid Red 18 dye adsorption on the physicochemical properties of silica precipitated in an emulsion route, used as a pigment and a filler in acrylic paints. Dyes & Pigments. 2003;57(1):29-41. https://doi.org/10.1016/S0143-7208(03) 00006-8.

[14] Yebra-Rodríguez A, Martín-Ramos JD, Del Rey F, Viseras C, López-Galindo A. Effect of acid

treatment on the structure of sepiolite. Clay Minerals. 2003;38(03):353-60. https://doi.org/10.1180/0009855033830101.

[15] Liu L, Chen H, Shiko E, Fan X, Zhou Y, Zhang G, et al. Low-cost DETA impregnation of acid-activated sepiolite for CO_2 capture. Chemical Engineering Journal. 2018;353:940-8. https://doi.org/ 10.1016/j.cej.2018.07.086.

[16] Cao L, Fei X, Zhang T, Yu L, Gu Y, Zhang B. Modification of C.I. Pigment Red 21 with Sepiolite and Lithopone in Its Preparation Process. Industrial & Engineering Chemistry Research. 2013;53(1):31-7. https://doi.org/ 10.1021/ie4021914.

[17] Giustetto R, Wahyudi O, Corazzari I, Turci F. Chemical stability and dehydration behavior of a sepiolite/indigo Maya Blue pigment. Applied Clay Science. 2011;52(1-2):41-50. https://doi.org/ 10.1016/j.clay.2011.01.027.

[18] Abbasian M, Jaymand M, Niroomand P, Farnoudian-Habibi A, Karaj-Abad SG. Grafting of aniline derivatives onto chitosan and their applications for removal of reactive dyes from industrial effluents. Int J Biol Macromol. 2017;95:393-403. https://doi.org/10.1016/j.ijbiomac.2016.11.075.

[19] Liu K, Chen L, Huang L, Lai Y. Evaluation of ethylenediamine-modified nanofibrillated cellulose/chitosan composites on adsorption of cationic and anionic dyes from aqueous solution. Carbohydr Polym. 2016;151:1115-9. https://doi.org/10.1016/j.carbpol.2016.06.071.

[20] Kumar MN, Muzzarelli RA, Muzzarelli C, Sashiwa H, Domb AJ. Chitosan chemistry and pharmaceutical perspectives. Chemical reviews. 2004;104(12):6017-84. https://doi.org/10.1002/chin.200511296.

[21] Darder M, López-Blanco M, Aranda P, Aznar AJ, Bravo J, Ruiz-Hitzky E. Microfibrous Chitosan−Sepiolite Nanocomposites. Chemistry of Materials. 2006;18(6):1602-10. https://doi.org/ 10.1021/cm0523642.

[22] El-Nahhal IM, Salem JK, Kuhn S, Hammad T, Hempelmann R, Al Bhaisi S. Synthesis & characterization of silica coated and functionalized silica coated zinc oxide nanomaterials. Powder Technology. 2016;287:439-46. http://dx.doi.org/10.1016/j.powtec.2015.09.042.

[23] Frindy S, Primo A, Qaiss Ael K, Bouhfid R, Lahcini M, Garcia H, et al. Insightful understanding of the role of clay topology on the stability of biomimetic hybrid chitosan-clay thin films and CO_2-dried porous aerogel microspheres. Carbohydr Polym. 2016;146:353-61. https://doi.org/ 10.1016/j.carbpol.2016.03.077.

[24] Zhou L, Jin J, Liu Z, Liang X, Shang C. Adsorption of acid dyes from aqueous solutions by the ethylenediamine-modified magnetic chitosan nanoparticles. Journal of hazardous materials. 2011;185(2-3):1045-52. https://doi.org/ 10.1016/j.jhazmat.2010.10.012.

[25] Travlou NA, Kyzas GZ, Lazaridis NK, Deliyanni EA. Functionalization of graphite oxide with magnetic chitosan for the preparation of a nanocomposite dye adsorbent. Langmuir : the ACS journal of surfaces and colloids. 2013;29(5):1657-68. https://doi.org/ 10.1021/la304696y.

[26] Laufer G, Kirkland C, Cain AA, Grunlan JC. Clay-chitosan nanobrick walls: completely renewable gas barrier and flame-retardant nanocoatings. ACS applied materials & interfaces. 2012;4(3):1643-9. https://doi.org/ 10.1021/am2017915.

[27] Hamdine M, Heuzey MC, Begin A. Effect of organic and inorganic acids on concentrated chitosan solutions and gels. Int J Biol Macromol. 2005;37(3):134-42. https://doi.org/10.1016/j.ijbiomac.2005.09.009.

[28] Zhu H-Y, Jiang R, Xiao L. Adsorption of an anionic azo dye by chitosan/kaolin/γ-Fe2O3

composites. Applied Clay Science. 2010;48(3):522-6. https://doi.org/10.1016/j.clay.2010.02.003.

[29] Huang R, Liu Q, Huo J, Yang B. Adsorption of methyl orange onto protonated cross-linked chitosan. Arabian Journal of Chemistry. 2017;10(1):24-32. https://doi.org/10.1016/j.arabjc.2013.05.017.

[30] Zhang Y, Fan L, Chen H, Zhang J, Zhang Y, Wang A. Learning from ancient Maya: Preparation of stable palygorskite/methylene blue@SiO_2 Maya Blue-like pigment. Microporous and Mesoporous Materials. 2015;211:124-33. https://doi.org/ 10.1016/j.micromeso.2015.03.002.

[31] Wang Q, Mu B, Zhang Y, Zhang J, Wang A. Palygorskite-based hybrid fluorescent pigment: Preparation, spectroscopic characterization and environmental stability. Microporous and Mesoporous Materials. 2016;224:107-15. https://doi.org/ 10.1016/j.micromeso.2015.11.034.

[32] Wu H, Gao G, Zhang Y, Guo S. Coating organic pigment particles with hydrous alumina through direct precipitation. Dyes and Pigments. 2012;92(1):548-53. https://doi.org/10.1016/j.dyepig.2011.06.014.

[33] Zhao X, Zhou S, Chen M, Wu L. Supramolecular architecture, spectroscopic properties and stability of C.I. Basic Violet 10 (Rhodamine B) at high concentration. Dyes and Pigments. 2009;80(2):212-8. https://doi.org/10.1016/j.dyepig.2008.07.003.

[34] Zhang G, Liu L, Shiko E, Cheng Y, Zhang R, Zeng Z, et al. Low-price MnO_2 loaded sepiolite for Cd^{2+} capture. Adsorption. 2019;25(6):1271-83. https://doi.org/10.1007/s10450-019-00132-3.

[35] Moreira MA, Ciuffi KJ, Rives V, Vicente MA, Trujillano R, Gil A, et al. Effect of chemical modification of palygorskite and sepiolite by 3-aminopropyltriethoxisilane on adsorption of cationic and anionic dyes. Applied Clay Science. 2017;135:394-404. https://doi.org/10.1016/j.clay.2016.10.022.

[36] Alcântara ACS, Darder M, Aranda P, Ruiz-Hitzky E. Polysaccharide–fibrous clay bionanocomposites. Applied Clay Science. 2014;96:2-8. https://doi.org/10.1016/j.clay.2014.02.018.

[37] Miura A, Nakazawa K, Takei T, Kumada N, Kinomura N, Ohki R, et al. Acid-, base-, and heat-induced degradation behavior of Chinese sepiolite. Ceramics International. 2012;38(6):4677-84. https://doi.org/ 10.1016/j.ceramint.2012.02.050.

[38] Fu S, Xu C, Du C, Tian A, Zhang M. Encapsulation of C.I. Pigment blue 15:3 using a polymerizable dispersant via emulsion polymerization. Colloids and Surfaces A: Physicochemical and Engineering Aspects. 2011;384(1-3):68-74. https://doi.org/10.1016/j.colsurfa.2011.03.009.

[39] Wilhelm P, Stephan D. On-line tracking of the coating of nanoscaled silica with titania nanoparticles via zeta-potential measurements. Journal of colloid and interface science. 2006;293(1):88-92. https://doi.org/ 10.1016/j.jcis.2005.06.047.

[40] Suárez M, García-Rivas J, García-Romero E, Jara N. Mineralogical characterisation and surface properties of sepiolite from Polatli (Turkey). Applied Clay Science. 2016;131:124-30. https://doi.org/10.1016/j.clay.2015.12.032.

[41] Li D, Qian L, Feng Y, Feng J, Tang P, Yang L. Co-intercalation of Acid Red 337 and a UV absorbent into layered double hydroxides: enhancement of photostability. ACS applied materials & interfaces. 2014;6(23):20603-11. https://doi.org/ 10.1021/am506696k.

[42] Valderrama C, Cortina JL, Farran A, Gamisans X, de las Heras FX. Evaluation of hyper-cross-

linked polymeric sorbents (Macronet MN200 and MN300) on dye (Acid red 14) removal process. Reactive and Functional Polymers. 2008;68(3):679-91. https://doi.org/10.1016/j.reactfunctpolym. 2007.11.005.

[43] Zhou Q, Gao Q, Luo W, Yan C, Ji Z, Duan P. One-step synthesis of amino-functionalized attapulgite clay nanoparticles adsorbent by hydrothermal carbonization of chitosan for removal of methylene blue from wastewater. Colloids and Surfaces A: Physicochemical and Engineering Aspects. 2015;470:248-57. https://doi.org/ 10.1016/j.colsurfa.2015.01.092.

[44] Ruiz-Hitzky E. Molecular access to intracrystalline tunnels of sepiolite. J Mater Chem. Journal of Materials Chemistry. 2001;11(1):86-91. https://doi.org/10.1039/B003197F.

[45] Wang Q, Feng Y, Feng J, Li D. Enhanced thermal- and photo-stability of acid yellow 17 by incorporation into layered double hydroxides. Journal of Solid State Chemistry. 2011;184(6):1551-5. https://doi.org/ 10.1016/j.jssc.2011.04.020.

[46] Dang L, Liang H, Zhuo J, Lamb BK, Sheng H, Yang Y, et al. Direct Synthesis and Anion Exchange of Noncarbonate-Intercalated NiFe-Layered Double Hydroxides and the Influence on Electrocatalysis. Chemistry of Materials. 2018;30(13):4321-30. https://doi.org/10.1021/acs.chemmater.8b01334.

[47] Hu X, Luo X, Xiao G, Yu Q, Cui Y, Zhang G, et al. Low-cost novel silica@polyacrylamide composites: fabrication, characterization, and adsorption behavior for cadmium ion in aqueous solution. Adsorption. 2020;1-12. https://doi.org/ 10.1007/s10450-020-00225-4.

[48] Fabjan EŠ, Saghi Z, Midgley PA, Otoničar M, Dražić G, Gaberšček M, et al. Diketopyrrolopyrrole pigment core@multi-layer SiO_2 shell with improved photochemical stability. Dyes and Pigments. 2018;156:108-15. https://doi.org/10.1016/j.dyepig.2018.03.064.

[49] Volle N, Giulieri F, Burr A, Pagnotta S, Chaze AM. Controlled interactions between silanol groups at the surface of sepiolite and an acrylate matrix: Consequences on the thermal and mechanical properties. Materials Chemistry and Physics. 2012;134(1):417-24. https://doi.org/10.1016/j.matchemphys.2012.03.011.

[50] Wu D, Hu L, Wang Y, Wei Q, Yan L, Yan T, et al. EDTA modified beta-cyclodextrin/chitosan for rapid removal of Pb(II) and acid red from aqueous solution. Journal of colloid and interface science. 2018;523:56-64. https://doi.org/10.1016/j.jcis.2018.03.080.

Conflict of interest

The authors declare that we do not have any commercial or associative interest that represents a conflict of interest in connection with the work submitted.

Credit author statement

Xiayi (Eric) Hu: Conceptualization, Writing - original draft, Writing - review & editing, Supervision, Funding acquisition, Project administration

Xuechun Feng: Writing - original draft, Writing - review & editing, Methodology, Experiment, Data curation.

Mingming Fei: Writing - review & editing.

Mi Tian: Writing - review & editing, Supervision.

Rui Zhang: Writing - review & editing, Supervision.

Yefeng Zhou: Writing - review & editing.

Yang Liu: Writing - review & editing.

Zhaogang Zeng: Writing - review & editing.